https://doi.org/10.1088/2631-8695/ab8e24

Printing Electronics Directly onto Carbon Fiber Composites: Unmanned Aerial Vehicle (UAV) Wings with Integrated Heater for De-Icing

Mohamad K. Idris[1], Jiefeng Qiu[2], Garrett W. Melenka[2], Gerd Grau[1]

[1] Department of Electrical Engineering and Computer Science, York University, Toronto, Canada
[2] Department of Mechanical Engineering, York University, Toronto, Canada

E-mail: grau@eecs.yorku.ca

Abstract

Unmanned Aerial Vehicles (UAVs) are increasingly used to deliver items and gather information in remote areas. As a result, UAVs suffer from ice accumulation on their wings, which drastically affects their flight. However, the UAV industry is still relatively young and, thus, commercial solutions for de-icing on UAVs are limited. The use of carbon fiber composites is becoming increasingly ubiquitous for UAVs as well as many other industries such as military, construction, medical, automobile, sporting goods and aircraft systems. Carbon fiber is commercially available in various forms, including single yarns, braids and weaves, which are similar to traditional textiles. This paper presents a method to create a self-heating composite structure that can be integrated into UAV wings for de-icing by exploiting the thermal and electrical conductivity of carbon fiber. Extrusion printing is used to fabricate electrical contacts directly on the carbon fiber weave. Extrusion printing on textiles faces multiple challenges that are overcome in this paper. A method is presented to extrusion print conductive paste on textiles. Specifically, carbon fiber weaves. This manufacturing method is employed to fabricate carbon fiber-based heating devices, and they are characterized electrically and thermally.

https://doi.org/10.1088/2631-8695/ab8e24

Keywords: Printed Electronics, Extrusion Printing, Woven Carbon Fiber Composites, De-icing Wings, Composite Heaters

1. Introduction

The use of unmanned aerial vehicles (UAVs) for information gathering and delivering items to remote areas has notably increased recently.[1] However, like passenger aircraft, ice accretion on wings is problematic for drones.[2] Aircraft icing occurs when water droplets from the air or clouds accumulate and freeze on the surfaces of an aircraft. Ice accretion greatly restricts the performance of aircraft. Ice accretion on the leading edge of a rotorcraft wing blade creates ice shapes that alter the lift, drag and pitching moment characteristics of the wing. In general, the performance of smaller aerial vehicles such as drones, commuter aircraft and small transport aircraft is more affected by icing than that of larger commercial transport aircraft due to their size. Just like rotorcrafts, ice accretion on the wings and tails of the aircraft reduces maximum lift and stall angle of attack, while increasing profile drag.[3] There are several methods for de-icing aircraft wings. De-icing fluids are commonly sprayed on aircraft before takeoff. Such de-icing fluids are usually water-based and include Freeze Point Depressants (FDP), mainly glycol, among other wetting agents and corrosion inhibiting materials.[4] In large commercial aircraft, the hot air produced from the engine is pumped through tubes into the inner surface of the wings.[2, 3] In smaller aircraft, electro-thermal systems can be used on surfaces such as intake lips or helicopter rotors.[3] However, due to its relatively young developing industry, commercially available solutions for de-icing of unmanned aerial vehicles are still limited.[5]

Carbon fiber is an attractive structural material because of its physical properties such as excellent tensile properties, low density, high strength to weight ratio, high thermal and chemical stability, and good thermal and electrical conductivity.[6] Carbon fiber is commercially available in various forms, including

single yarns, braids and weaves (e.g. Unidirectional or Twill as shown in Figure 1 (a)). These carbon fiber textiles are treated with epoxy to combine the physical properties of carbon fiber and epoxy to create woven carbon fiber composites. The epoxy allows the composite to maintain its structure and shape as carbon fiber is only strong in tension, not shear or compression. Carbon fiber composites have been in heavy demand recently for industries such as the military, construction, medical, automobile, sporting goods and aircraft systems, including UAVs.[7] Carbon fiber composites can be used as tubes connecting the body of a drone to its rotors,[8] or to create the propellers and wings of a UAV.[9] The fact that carbon fibers are electrically and thermally conductive means that they can be directly used as the heating element in an electric heater. This way, an aircraft wing can be heated without the need for a separately applied heater, such as a flexible heater on a plastic substrate. This reduces the complexity of integrating a de-icing system into a UAV and reduces cost since the heating element, i.e. the structural carbon fiber does not need to be added separately to the system. There are successful reports of creating heaters using graphene, carbon nanotubes and carbon fiber using different methods. One method combines a matrix of carbon fiber pre-impregnated with epoxy (pre-preg) with highly aligned carbon nanotube webs produced by chemical vapor deposition (CVD) and copper foil busses for connections.[10] Another method uses a combination of graphene films and carbon fiber reinforced polymer (CFRP) laminates and copper electrodes.[11] Other methods create de-icing heaters using individual carbon fiber tows either impregnated with epoxy for 3D printing or as wires embedded into concrete.[12–14] However, these methods add complex processes or expensive materials to the manufacturing process. They generally don't make use of the same carbon fiber textiles commonly used as a structural material nowadays. Here, we propose to use these textiles as the heating element without major changes to common CFRP manufacturing processes, which requires electrical contacts to be fabricated directly on the carbon fibers.

There are multiple ways to create electronic textiles (e-textiles), including sewing and knitting, weaving, braiding, coating/laminating, chemical treatment and printing.[15] Printing is a promising method because

it is low-cost, scalable and enables the rapid customization of designs using digital printing technology. We estimate the added cost per unit area of manufacturing. The proposed carbon fiber heater is only 0.03$/cm2.

Printed electronics is becoming increasingly viable and is considered a key technological enabler for the Internet of Things (IoT) due to its potential for mechanical flexibility, low weight, low cost, ecofriendly, on-demand printability and scalability.[16] Multiple printing techniques have been proposed for printed electronics, including inkjet printing, screen printing, gravure printing, and extrusion printing.[17] Inks for such printing techniques can be based on a variety of materials, including metal particles or organic materials, to print conductors, insulators and semiconductors.

Printing organic electronics on textiles is very interesting because it allows for the integration of the enhanced functionality of electrical elements and the physical properties of textile materials.[18] However, textiles are usually porous and have high surface roughness, thus presenting multiple challenges for the various printing methods.

So far, screen printing has been the most effective and most widely used method to print on textiles. Screen printing is a high-volume mask-based technique. The design of the print is patterned as a mask on a mesh. The ink is spread over the mesh and pushed through it using a squeegee, thus creating a pattern on the substrate. This technique is ideal for printing on a large scale on a range of materials including textiles, glass, wood and ceramics.[19] Screen printing is commonly used in printed electronics to print interconnects and passive circuit elements.[20] Screen printing creates thick-layer patterns using high-viscosity inks, which can overcome the roughness of the textile.[15, 19] Nevertheless, screen printing wastes substantial ink in the process, which, in the case of printing electronics, is not cost-effective due to the expensive materials used in the inks. Also, it requires a pre-designed mask, which can prove costly if it is required to modify the printing pattern constantly.

Inkjet printing has also been used to print on textiles. Inkjet printing is a non-contact digital additive technique that can deposit ink on various substrates. Droplets are jetted from a nozzle towards the substrate following a pre-designed layout without using any masks or etching processes, which can make it more cost-effective than screen printing on textiles, especially for low-volume applications.[21] This technique has been used to print various microelectronic devices such as organic thin-film transistors (OTFT), organic light-emitting diodes (OLED) and organic solar cells (OPV).[22, 23] However, the inks used for inkjet have very low viscosities. As a result, to inkjet print on textiles, an interface layer is required to reduce surface roughness and ensure pattern continuity, which is critical for electronics. The interface layer is usually appliedto the textile using dip coating, spin coating or even screen printing.[15, 18, 21, 24]

Extrusion printing, also known as dispenser printing, works by applying pressure to dispense ink through small nozzles, as shown in Figure 1 (b). This technique has multiple parameters, including ink viscosity, nozzle diameter, nozzle height offset from the substrate, print speed and most importantly, pressure control. Depending on the ink and substrate material, there is an optimal combination of these parameters for printing. Extrusion printing is commonly used to print metal-based inks, mostly silver, which consist of metal flakes and a polymer binder dissolved in a solvent.[25] Inks for extrusion printing are high viscosity (approximately 10^3 to 10^6cP) to prevent leakage through the nozzle.[26] Extrusion printing is considered a digital printing technique that can be used to print flexible and stretchable interconnects and passive circuit elements.[27] Extrusion printing combines the positive attributes of both inkjet and screen printing when used for printing on textiles. It is a contactless nozzle-based method, it is a digital method that does not require a mask, ink is extruded only when needed, and it can print highly-viscous inks to create thick-layer patterns which is ideal for printing on textiles.

Extrusion printing faces many challenges when used to print on textiles, chief among is the fact that it requires the nozzle to be very close to the substrate. When the nozzle is close to the substrate, it can get

entangled in the fibers of the textile, thus, either moving and destroying the substrate or damaging the delicate nozzle. So far, no successful extrusion printing attempts on textiles have been reported.

There have been successful attempts of printing electronics on carbon fiber reinforced polymers (CFRP) using aerosol-jet and inkjet printing to create strain sensors for composites.[28–33] However, no successful attempts have been reported to print electronics on dry carbon fiber weaves without the epoxy matrix. Printing directly on dry carbon fibers offers two important advantages. One, the printed silver can make direct contact with the electrically conducting carbon fibers without insulating epoxy in between. This ensures good electrical conduction to the fibers. Two, the silver can be printed on the carbon fiber textile in the flat state without difficulties due to potentially complex 3D geometry. Subsequently, the textile will acquire its final shape when it is infused with epoxy, e.g. in the form of an aircraft wing.

This paper presents a method to use extrusion printing to print electronics on textiles; specifically carbon fiber weaves. This paper also exploits the thermal and electrical conductivity of carbon fiber to create a self-heating composite structure using extrusion printing. The resultant heating device could be integrated into UAV wings for de-icing.

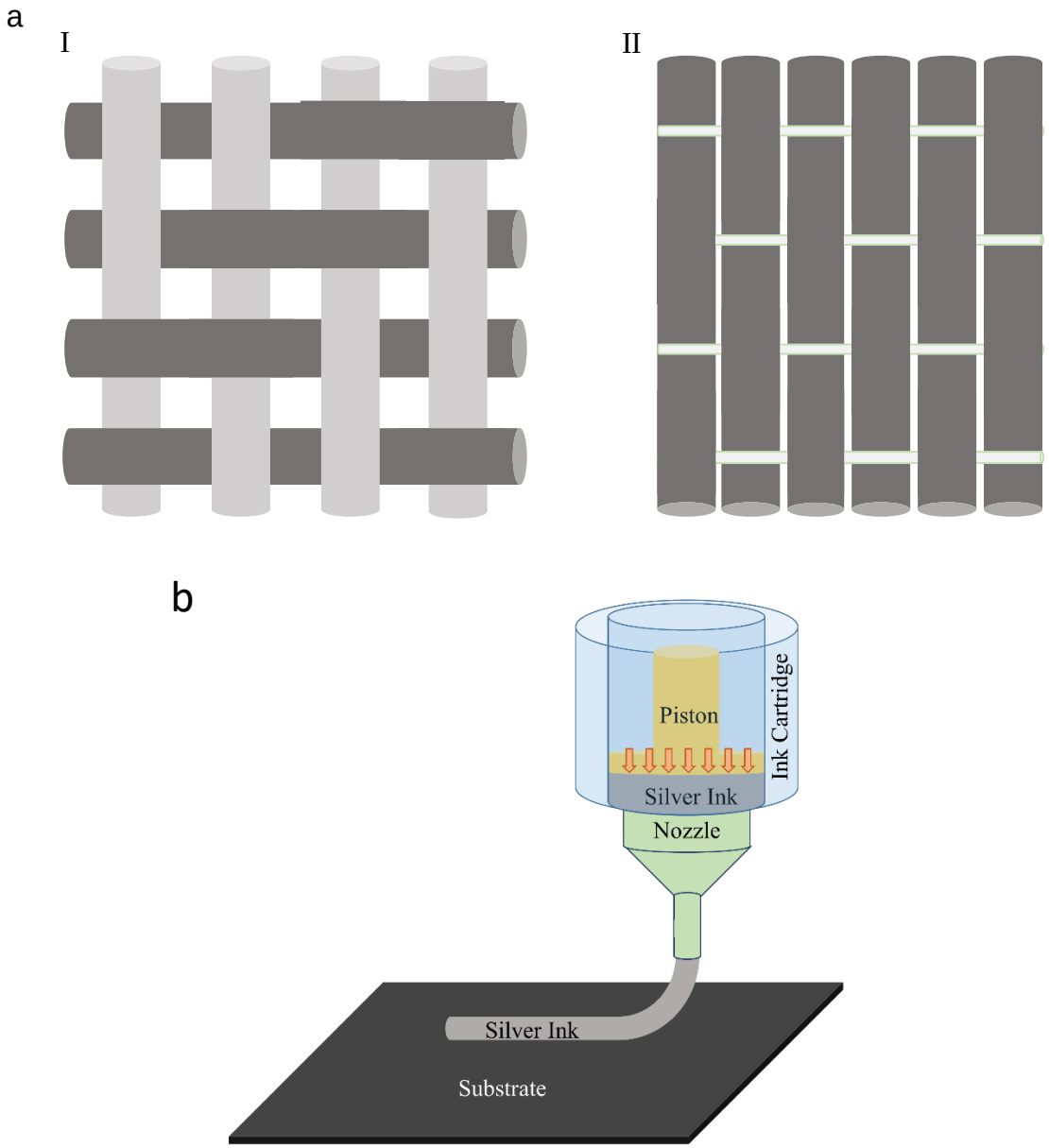

Figure 1. a) Illustration of different forms of carbon fiber weaves: I) Twill (2x2) weave with orthogonal fiber tows crossing over each other, II) Unidirectional weave with carbon fiber tows in only one direction; b) Illustration of the extrusion printing process. The piston applies pressure to the ink, which is dragged out of the nozzle as it translates relative to the substrate.

2. Methods

2.1. Materials

Three different types of weaves were used: 12K Unidirectional weave (12K UD), 6K Twill weave and 3K Twill weave. The weaves have different thicknesses due to the different number of fibers in each tow (12K, 6K and 3K), which is essential information for extrusion printing. The Unidirectional and Twill weaves have different geometries. In the Unidirectional case, all carbon fibers are aligned in the same direction with no fibers crossing over each other. Twill weaves have orthogonal carbon fiber tows crossing over each other with a periodicity of two tows (2x2 Twill). See Figure 1 (a) for an illustration. The different geometries affect the electrical current and heat flow. Unidirectional limits current and heat flow to one direction aligned with the carbon fiber tows. The carbon fiber weaves were acquired from Sigmatex Ltd. The weaves were infused with 2000 laminating epoxy resin system 9 (Fibre Glast 2000 laminating and 2020 hardener). This epoxy is a room temperature two-part system that is used in the production of high strength structural parts in the space, automotive and structural industries.

LOCTITE Frekote 700-NC was used as a release layer on the mold plates and the 3D printed wing before putting the carbon fiber weave on them to create multiple interfacing layers that prevent the epoxy from sticking to the mold.

Extrusion printing on carbon fiber was achieved using a desktop printed circuit board printer (Voltera V-One PCB printer, Kitchener, ON). The nozzle size was 225 µm. The ink was a silver flake ink (120-07) from Creative Materials Inc. This ink's viscosity (26,000 - 30,000 cP) is high enough for extrusion printing. The printing pattern was designed using EAGLE, Autodesk.

2.2. Printing on Carbon Fiber

The V-One printer utilizes multiple steps for the printing process: probing, ink calibrating and printing. A sharp tip is used to probe the surface of the substrate in contact mode to determine its position and

height. This ensures consistency in print height and prevents the delicate nozzle tip from hitting the substrate and breaking in the printing phase. In the ink calibration phase, the cartridge is mounted, and the printer prints a built-in design on a dummy substrate. The various printing parameters can be edited until the desired amount of ink is dispensed. In the printing phase, the pattern design is printed on the substrate by scanning the nozzle and controlling the pressure in the ink cartridge with a piston. Using this method and printer to print on carbon fiber weaves presents multiple challenges. The contact-based probe cannot be used with the textile as it can either bend the fibers and break them or penetrate between the fiber tows. Therefore, instead of probing the carbon fibers directly, the nozzle height above the underlying glass substrate was increased by the average thickness of the carbon fiber textile measured using a micrometer (Power Fist 0-1”). Additionally, the weave has large surface roughness and topography, and there are a large number of frayed fibers and tows, which can cause the nozzle to get entangled. To overcome this challenge, tension is applied to the carbon fiber weave when clamping it down. Then, the weave is sprayed with acetone until saturated which mechanically pushes down the tows, and the frayed fibers stick to the glass slide due to surface tension. After waiting for approximately 5 minutes to ensure that the acetone has fully evaporated and the weave has dried, the printing phase is initiated. An additional offset of 350μm is added to the nozzle height above the nominal surface of the carbon fiber weave to prevent nozzle entanglement. The height offset is the minimum offset possible to print on the weave. As a result, the printing parameters had to be adjusted to print at this extreme nozzle height as discussed in the discussion section below. Finally, the pattern is successfully printed on the carbon fiber weave. This method can potentially be used to print on a wide range of textiles that have similar or lower surface roughness than the carbon fiber weaves used here.

2.3. Heating Device Manufacturing

Manufacturing the heating device is done in four steps. First, the designed silver pattern is printed on a 2D flat and dry carbon fiber weave, as shown in Figure 2 (a). The weave is then put into a gradually heating oven at 150º C for 30 minutes to cure the printed silver. Then, the epoxy is mixed at the recommended ratio (4:1 Resin: Hardener) and infused into the carbon fiber weave, as shown in Figure 2 (b). In the third step, flat 2D and 3D devices are made. For the flat 2D devices, the weave is positioned between two polished stainless-steel plates. A mechanical press is used to apply pressure (3 tons of force) on the plates to push out excess epoxy resin and give a smooth finish to the carbon fiber composite, as shown in Figure 2 (c). The release layer is applied on the plates before putting the carbon fiber weave on them to prevent the epoxy from sticking to the mold. The epoxy resin infused weaves were left to cure at room temperature for 24 hours. Finally, the carbon fiber composite is delaminated from the plates, as shown in Figure 2 (d). In the case of the 3D devices, the first two steps are repeated (printing silver onto CF and infusing with epoxy). In the third step, a Clark-Y wing is 3D printed and used as a mold. This wing design was selected for this proof of concept because it is commonly used in small aircraft. It also has a smooth profile with curvature within the bending limits of the cured silver contacts. The carbon fiber weave is wrapped over the mold, and pressure is applied using heat-shrink tape wrapped over the weave, as shown in Figure 2 (e). The release layer is applied on the 3D printed wing before putting on the carbon fiber weave to prevent the epoxy from sticking to the mold. The epoxy resin infused weaves are left to cure in room temperature for 24 hours. The final 3D wing is shown in Figure 2 (f). The epoxy covering the printed silver electrodes is burnt off using a soldering iron at 450º C in strategic locations, making it possible to connect to the silver electrodes.

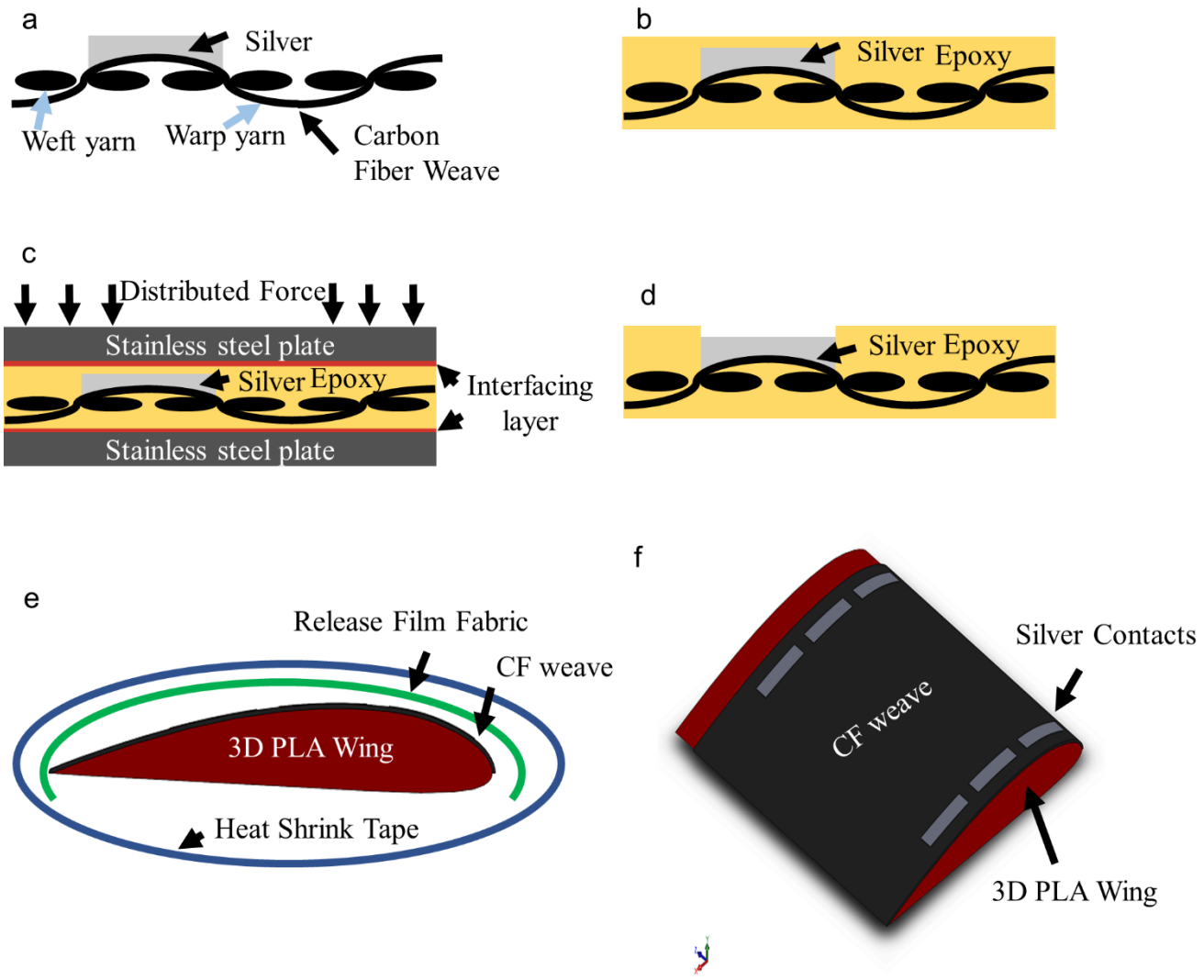

Figure 2. Heater Manufacturing Steps. a) Print pattern on dry carbon fiber weave (cross section); b) Infuse weave with epoxy. For flat device: c) Apply force and cure device in room temperature; d) Peal off, then melt epoxy covering silver pads. For 3D device: e) Wrap carbon fiber weave around mold and apply force using heat-shrink tape; f) Remove tape and then melt epoxy covering silver pads.

2.4. Characterization

The profiles of printed lines on glass were measured using stylus profilometry (Alpha-Step D-500, KLA Tencor). Electrical measurements and current injection for the heaters were performed using a DC current-voltage source measure unit (KEITHLEY 2602B SYSTEM SourceMeter®). Heat images were obtained with an infrared camera (FLIR A6751sc).

3. Results and Discussion

3.1. Designing the Pattern

Silver electrodes are printed on the carbon fiber weaves to produce a large-area heater. The electrodes are used to run an electrical current through the weaves resulting in power dissipation in the form of heat. It is essential to design the device for maximum power consumption and heat generation in the carbon fiber rather than the silver contacts to achieve maximum power efficiency. Three main parameters were considered to design the printing pattern: The width of the silver electrodes (W_{Ag}), the length of the silver electrodes (L) and the distance between the two electrodes (W_{CF}) as shown in Figure 3 (a). As voltage is dropped over the electrodes, the voltage across the carbon fiber heater diminishes with increasing distance from the point of current injection (distance x in Figure 3 (a)). Consequently, the electrical power dissipated in the carbon fiber, which is converted to heat, is lowest at the opposite end of the electrodes (x=L). To quantify this non-uniformity, we calculate the efficiency at the end of the electrodes (P(L)%) i.e. the power consumed in the carbon fiber per unit width and converted to heat at x=L as a percentage of the power consumed at x=0. The silver electrodes and the carbon fiber weave are treated as distributed resistances and the differential equations relating voltage and current as a function of position is solved to calculate the efficiency of the heater as a function of electrode length as shown in equations (1-3). The full derivation can be found in the supplementary information. R_{Ag} is the resistance of the silver electrode per unit length and R_{CF} is the resistance of the carbon fiber weave per unit width. t_{Ag} and t_{CF} are the thicknesses of the silver electrodes and carbon fiber weave respectively. ρ_{Ag} is the electrical resistivity of the silver electrodes and ρ_{CF} is the resistivity of the carbon fiber.

$$R_{Ag} = \rho_{Ag}/(t_{Ag} \times W_{Ag}) = 3 \times 10^{-3}\Omega \, / \, W_{Ag} \quad (1)$$

$$R_{CF} = \rho_{CF} \times W_{CF}/t_{CF} = 3.3 \times 10^{-2}\Omega \times W_{CF} \quad (2)$$

$$P(L)\% = \frac{4\,exp\left(2L\sqrt{2R_{Ag}/R_{CF}}\right)}{\left(1+exp\left(2L\sqrt{2R_{Ag}/R_{CF}}\right)\right)^2} \quad (3)$$

As shown in Figure 3 (b), (c) and (d), the efficiency increases with increasing width of the silver electrodes (W_{Ag}) and distance between the two electrodes (W_{CF}). At the same time, it decreases with increasing length of the silver electrode (L). Better efficiency is achieved when the resistance of the silver electrodes is small compared with the resistance of the carbon fiber heating element because these resistances are connected in series acting as a voltage divider. By maximizing the resistance of the carbon fiber heater relative to the resistance of the electrodes, it is ensured that more of the input voltage and power are dropped across the heater rather than the electrodes. This design assumes the current is injected from one side of the electrodes. However, injecting the current in the middle of the electrodes allows for doubling the length of the electrodes (L), hence, creating a larger area heating device. The printing area of the V-One printer limits the maximum extent of WCF. Considering this, the design dimensions were set to W_{Ag} = 5 mm, W_{CF} = 100 mm and L = 10 mm (from midpoint of electrode) as shown in Figure 3 (e) giving an efficiency of 96%. Further improvements will be possible with a larger print area and thus larger W_{CF}. Printing multiple silver layers could also potentially improve efficiency by increasing silver thickness t_{Ag}, reducing R_{Ag} and consequently increasing P(L)% according to equations (1) and (3).

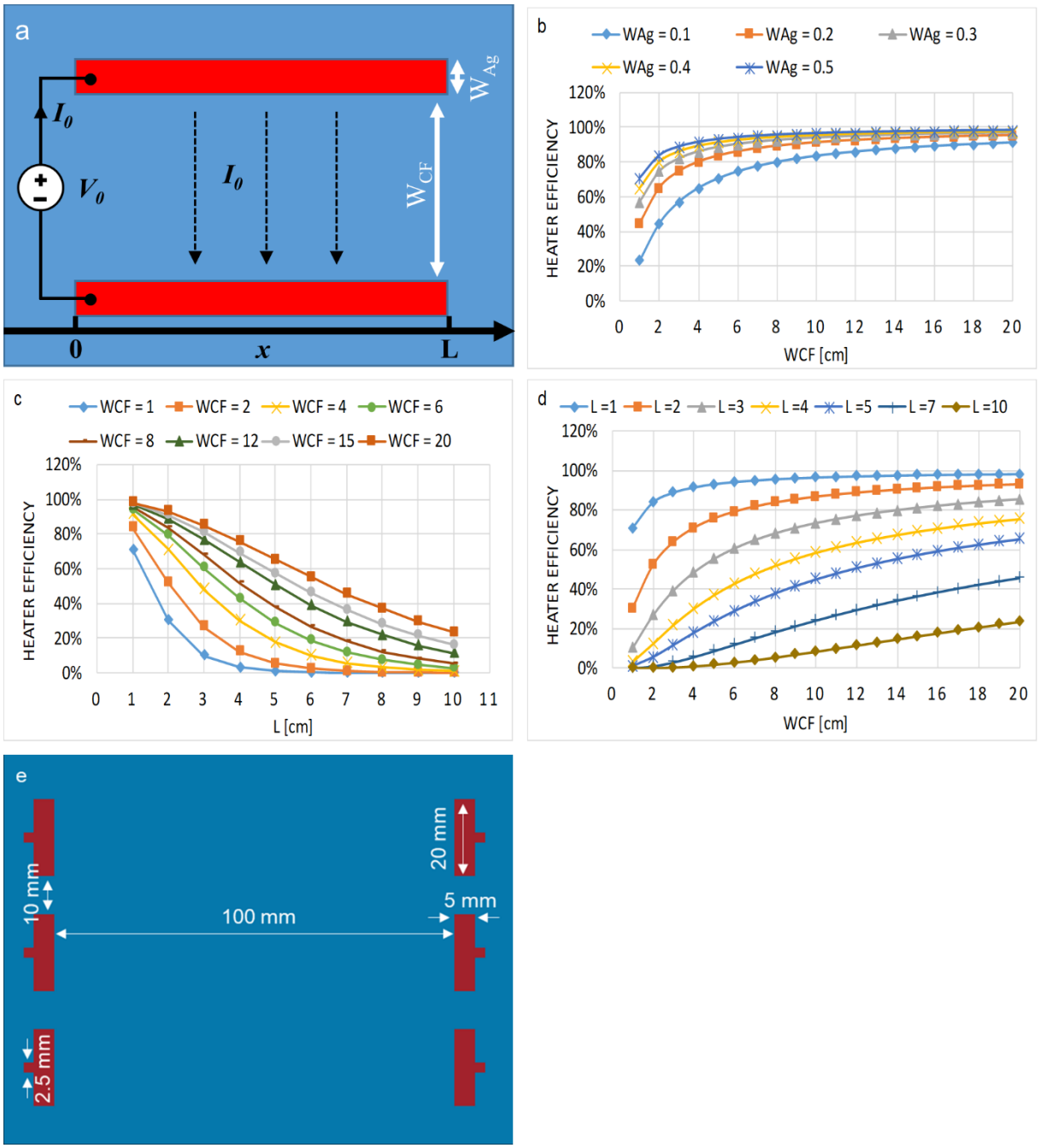

Figure 3. a) Printing pattern design parameters and electrical configuration with current injection on one side at x=0. Coordinate x is defined along the length of electrodes. b)-d) Effect of the three different design parameters on power efficiency (all units in legends in cm): b) L held constant at 1 cm; c) W_{Ag} held constant at 0.5 cm; d) W_{Ag} held constant at 0.5 cm. e) Printing pattern design and dimensions of the final heater in EAGLE containing three heaters arranged vertically. Current is injected into the pads at the center of the electrodes and flows horizontally.

3.2. Printing Parameters

Printing using the Voltera V-one printer has multiple printing parameters. Lines and squares were printed on glass to optimize these parameters while considering the constraints of the carbon fiber weaves, as shown in Figure 4 (a). The printed features were analyzed using a stylus profilometer, as shown in Figure 4 (b). Then, optimized parameters, shown in Table 1, were used to print on the carbon fiber weaves.

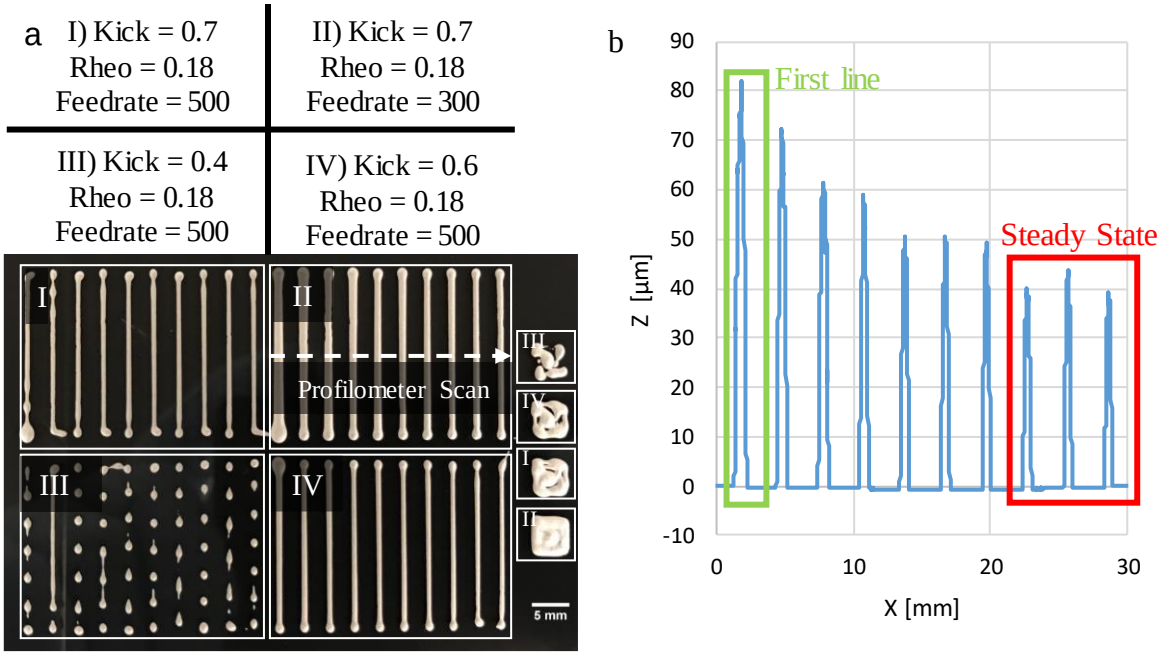

Figure 4. a) Line and square patterns printed on glass slide at a nozzle height offset of 350 µm. One can observe discontinuous lines when printing parameters are close to the default values (III). Increasing Kick increases the dispensed ink volume but ink volume diminishes during the print if Rheological Setpoint is not increased as well (I, II, IV). In each print, the line on the left was printed first. Decreasing Feedrate leads to wider and thicker lines (II). b) Profilometry scan across printed lines with parameters: Nozzle height=350 µm, Kick=0.7 mm, Rheological Setpoint=0.18, Feedrate=300 mm/min. X represents distance along the profilometer scan across multiple lines starting with the line that was printed first at X=0 (see arrow in (a) (II) indicating orientation of profilometer scan). Z represents measured height profile of the printed lines. Cross-sectional area (ink volume per unit length) diminishes from first line until steady state is reached.

The most relevant printing parameters that were studied are: Dispense height, Kick, Rheological Setpoint (Rheo) and Feedrate. Dispense height corresponds to the nozzle height offset from the substrate.

Increasing the nozzle height results in a decrease in ink per unit length of lines (cross-sectional area of lines in profilometry scan) dispensed in steady state as shown in Figure 5 (a). This is a major problem for printing onto carbon fiber weaves, where a large nozzle height is required due to the uneven topography of the weave and to prevent the nozzle from getting entangled in stray fibers. The other printing parameters need to be adjusted to compensate for this problem. Kick and Rheological Setpoint control the pressure in the cartridge, thus controlling the amount of dispensed ink. The Kick parameter controls the stroke length of the dispensing piston. Increasing the Kick results in an increase in ink dispensed overall and especially in the first line, as shown in Figure 5 (b). This can overcome the reduction in ink flow due to the increased print height. However, the increased ink flow diminishes over time for larger prints. For example, when multiple lines are printed successively, later lines will have less ink (see Figure 4 (b)). This is a problem when trying to print repeatable patterns over large areas such as on an aircraft wing. The Rheological Setpoint parameter needs to be adjusted to achieve repeatable patterns on a large area. The Rheological Setpoint corresponds to how the printer compensates for the flow rate over time. After the initial piston stroke (corresponding to the Kick), the piston is pulled back a fraction to release pressure and ensure steady ink flow despite of the viscoelastic nature of the ink/paste that is printed. Increasing the Rheological Setpoint reduces this pullback resulting in more ink flow over time throughout the print. Therefore, increasing the Rheological Setpoint increases compensation for ink flowing out of the cartridge during the print and thus the amount of ink dispensed for every line as shown in Figure 5 (c) and (d). Feedrate corresponds to the nozzle XY-axis travel speed during dispensing. Increasing the Feedrate results in less ink per unit length of line as shown in Figure 5 (e). This means there exists a trade-off between manufacturing throughput and line thickness. Above a threshold of 500 mm/min, lines were not continuous anymore. In addition to lines, squares were also printed and analyzed in terms of defects (holes). The dispensed ink volume follows the same trends and the same optimized printing parameters can be used.

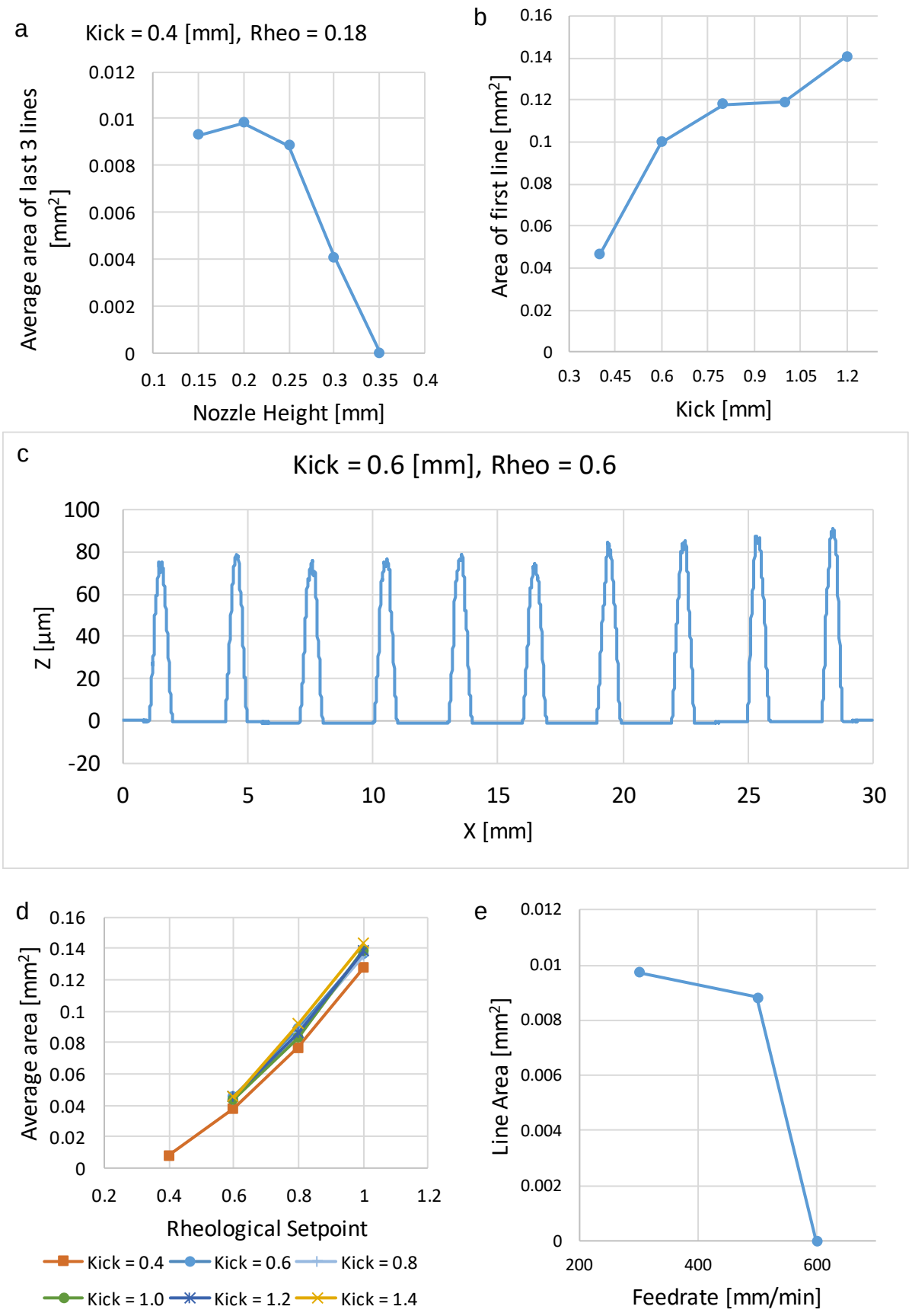
a
Kick = 0.4 [mm], Rheo = 0.18
Average area of last 3 lines [mm²]
0.012
0.01
0.008
0.006
0.004
0.002
0
0.1 0.15 0.2 0.25 0.3 0.35 0.4
Nozzle Height [mm]
b
Area of first line [mm²]
0.16
0.14
0.12
0.1
0.08
0.06
0.04
0.02
0
0.3 0.45 0.6 0.75 0.9 1.05 1.2
Kick [mm]
c
Kick = 0.6 [mm], Rheo = 0.6
Z [µm]
100
80
60
40
20
0
-20
0 5 10 15 20 25 30
X [mm]
d
Average area [mm²]
0.16
0.14
0.12
0.1
0.08
0.06
0.04
0.02
0
0.2 0.4 0.6 0.8 1 1.2
Rheological Setpoint
Kick = 0.4
Kick = 0.6
Kick = 0.8
Kick = 1.0
Kick = 1.2
Kick = 1.4
e
Line Area [mm²]
0.012
0.01
0.008
0.006
0.004
0.002
0
200 400 600
Feedrate [mm/min]

Figure 5. a) Effect of nozzle height on line area. Increasing nozzle height, as required to print onto rough carbon fiber weave, results in diminished ink flow with standard settings. b) Effect of Kick on line area. Increasing Kick increases ink flow; however, predominantly for the first line in larger prints. c) With higher Rheological Setpoint, diminishing ink flow during longer prints is compensated for resulting in more uniform printing. d) Effect of Rheological Setpoint parameter on steady state line area. e) Effect of Feedrate on line area. The maximum Feedrate that gives working lines is 0.5 m/min.

The insights gained by printing onto glass also apply to printing onto carbon fiber weaves. Figure 6 (a) shows the same trends for individual lines. Kick and Rheological Setpoint need to be increased from default values to achieve consistent printing of sets of lines with the increased print height necessary to print onto rough carbon fiber weaves. Continuous lines can be achieved; however, pattern fidelity is deteriorated because of the topography of the carbon fiber weave. Bulges occur where the printed lines cross from one carbon fiber tow to the next or cross over the nylon yarns holding the unidirectional weave together. In order to achieve good pattern fidelity and heater efficiency, as discussed in section 3.1, 5 mm wide heater contacts were printed onto the carbon fiber weaves. On carbon fiber, the printing parameters that were optimal on glass resulted in a small excess of ink dispensed, which resulted in some parallel lines connecting with each other. As a result, the dispensing pressure was decreased one step to Kick = 0.5 mm and Rheological Setpoint = 0.5. The optimized print parameters to print these contacts on CF are shown in Table 1. Figure 6 (b)-(f) show the final heater devices with printed heater contacts on the different carbon fiber weaves (12K UD, 6K Twill, 3K Twill) as well as on the 3D wing structure.

Table 1. Optimized printing parameters used in heater manufacturing.

Nozzle offset from carbon fiber weave	350 µm
Kick	0.5 mm
Rheological Setpoint	0.5
Feedrate	500 mm/min

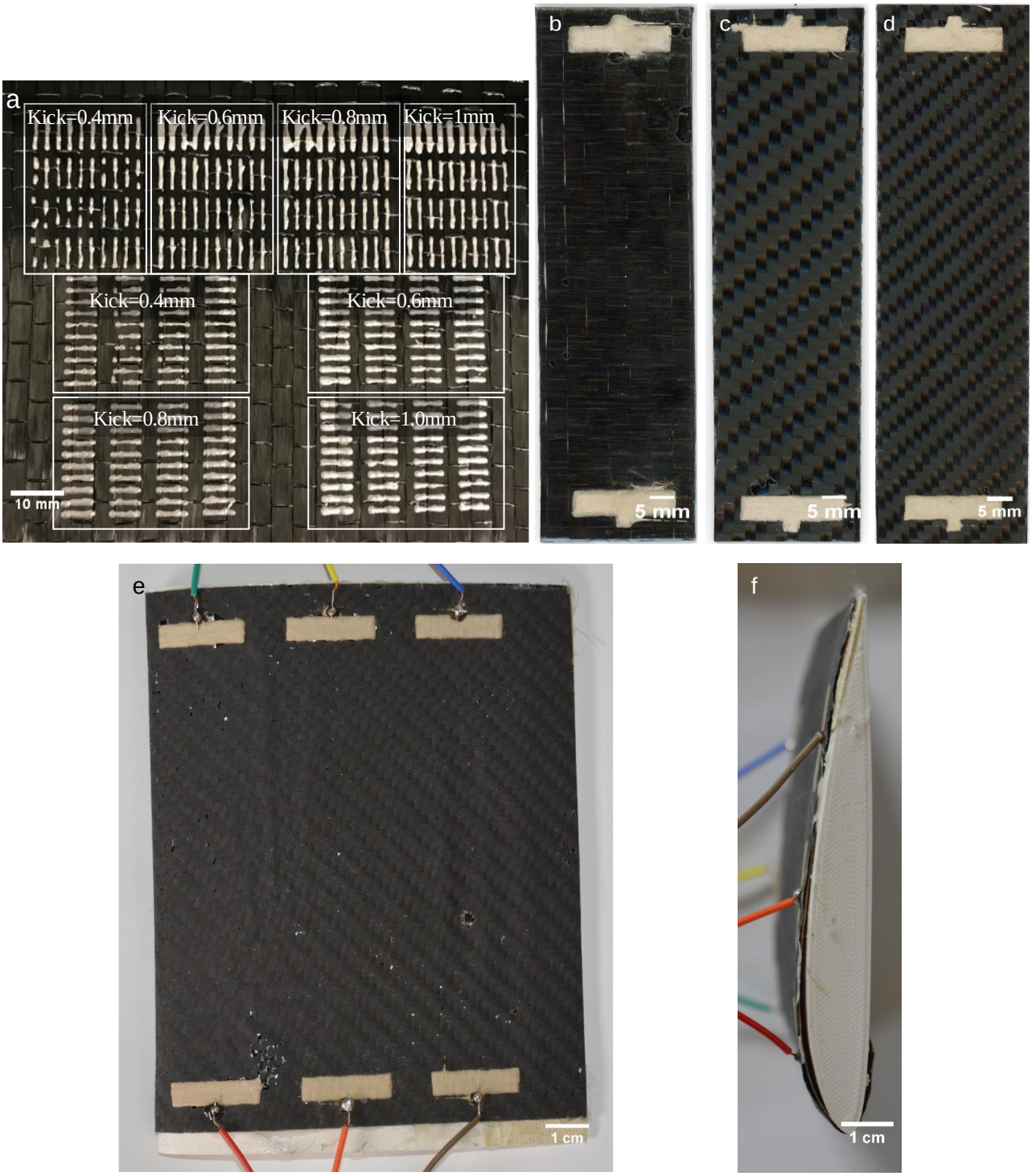

Figure 6. Printed silver electrodes on carbon fiber weaves. a) Blocks of individual lines printed on 12K UD carbon fiber in two directions using different Kick and Rheological Setpoint values. Rheo values from top to bottom and left to right: 0.4, 0.5, 0.6, 0.8. Similar trends can be observed as on glass. Lines can be continuous, but pattern fidelity is deteriorated by topography of CF weave. b) Fully manufactured flat heater device using 12K UD carbon fiber weave. c) Fully manufactured flat heater device using 6K Twill carbon fiber weave. d) Fully manufactured flat heater device using 3K Twill carbon fiber weave. e) Three fully manufactured 3D heater devices on a wing mold with 3K Twill. f) Profile of 3D wing with integrated heaters.

3.3. Electrical and Heat Measurements

After the flat devices were manufactured, their electrical resistance was measured using the 4-point probe technique.[34] The resistance measurement for all samples was approximately 1.1Ω. Furthermore, the devices were connected to a current source, and an infrared camera was used to measure the temperature of the device. The amount of heat produced by the device corresponds to the electrical power consumed in the carbon fibers, which is proportional to the resistance of the device and the square of the input current. A current sweep was applied to all devices. Figure 7 (a) shows that the device could go as high as 108ºC using a 3A current source, which is more than enough for de-icing. Lower current levels can likely be used to save energy depending on the severity of the ice conditions; however, this may not be necessary if de-icing is done on the ground with access to external power. Figure 7 (b), (c), (d) show that the orientation of the carbon fiber weave and the number of fibers in each tow influence the current and heat flow in the device. The Unidirectional weave (12K UD) exhibits a high degree of anisotropy. Electrical current is conducted along individual fiber tows, but conduction is minimal across different tows. Similarly, heat is not conducted well between tows. Tows are aligned with the direction of current flow to achieve electrical conduction between the electrodes. As a result, a hot zone can be observed at the center of the device with cold zones at the edges. The heat does not spread uniformly over the Unidirectional weave. Conversely, the Twill weaves have carbon fibers running in two orthogonal directions. The electrodes are printed such that one set of fiber tows is aligned with the direction of electrical current flow. Heat can spread along orthogonal fibers leading to a much more uniform heat distribution. 3K Twill has smaller fiber tows than 6K Twill, which again gives a more uniform heat distribution. Aheater with long electrodes (10 cm) was also printed to confirm the modelling in section 3.1 and as expected did not perform well. Only minimal heating can be observed close to the point of current injection on the right side of Figure 7 (e). Finally, a current of 3A, which was the limit of our current source, was supplied to the 3D wing containing three separate heaters (1A per heater), and the heat

images were taken using the same apparatus used for the flat 2D devices. The temperature at the center of the wing reached 35°C, which is comparable to the individual flat heaters for the same current of 1A per heater. Figure 7 (f) shows the temperature distribution in the 3D wing device and Figure 7 (g) shows the temperature distribution at the center of the wing away from the electrodes. Some non-uniformity can be observed corresponding to the three heater devices. This could potentially be improved by optimizing the electrode geometry further, for example by placing electrodes closer to each other. Current and heat crowding close to the electrodes is more apparent in the larger CF sheet of the wing compared with individual flat heaters, but this does not significantly affect heating at the center of the wing where the de-icing would occur.

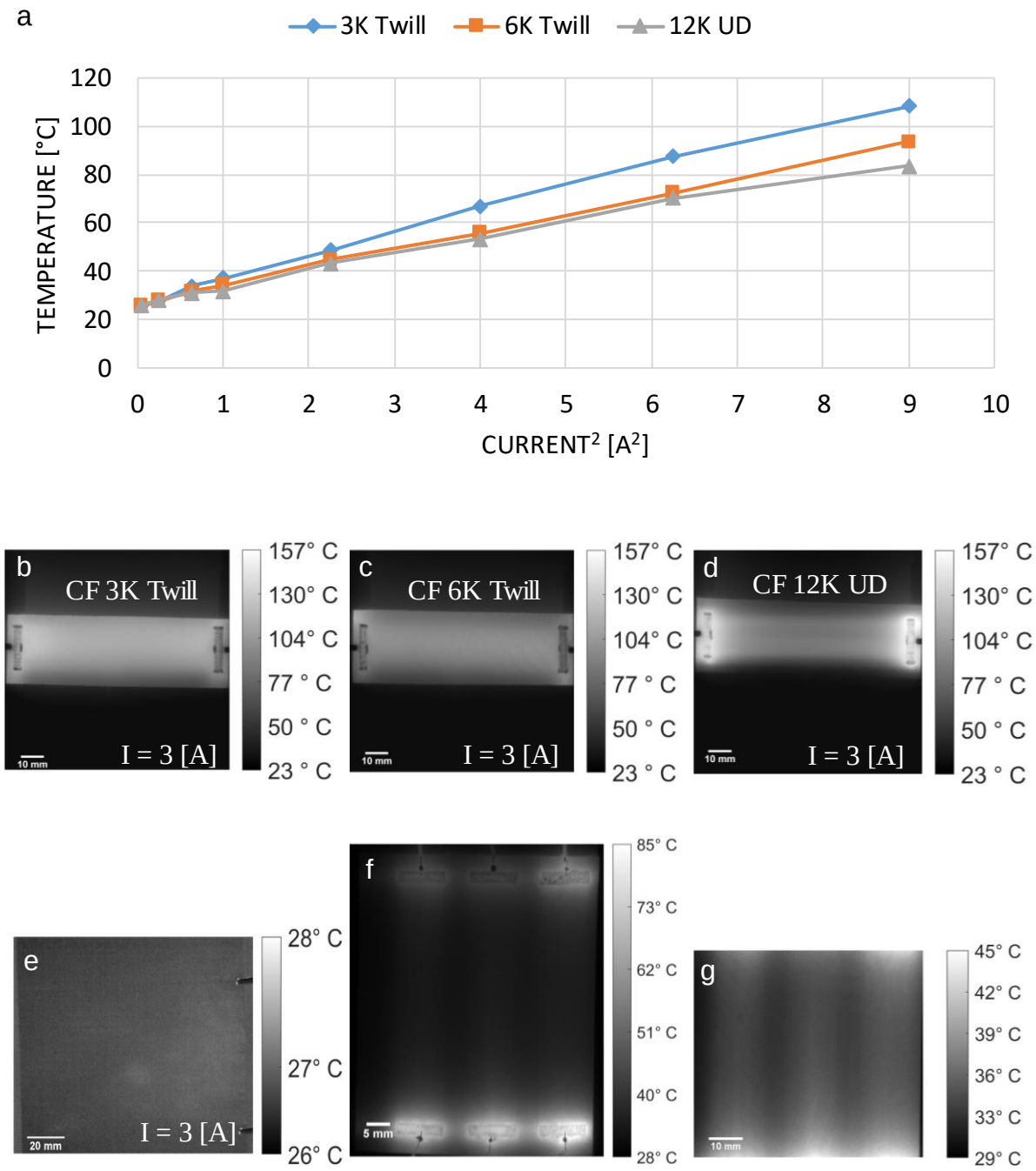

Figure 7. a) Heater temperature increases with the square of electrical current as expected for Joule heating. Temperature was averaged over a region of interest at the center of the heater (2cm x 2cm). b) IR image of 3K Twill CF weave exhibiting good uniformity. c) IR image of 6K Twill CF weave. d) IR image of 12K UD CF weave exhibiting reduced uniformity. e) IR image of wide heater with single set of two long electrodes extending horizontally across the sheet (L = 10cm). Only minimal heating close to the point of current injection (right) can be observed. f) IR image of 3D wing using 3K Twill CF weave with 1A of current per heater. g) IR image of the center region of the 3D wing shown in (f). The entire wing is heated with some temperature non-uniformity in between heaters.

4. Conclusion

This work exploits the electrical and thermal conductivity of carbon fiber to create self-heating composites that could be integrated into UAVs for de-icing. The manufacturing of the integrated heating devices is based on commonly used composites manufacturing methods with the addition of a printing step to create electrical contacts. The devices were manufactured, and temperature measurements were taken using an IR camera. Results show that the heating devices have been successfully fabricated and can achieve high temperatures suitable for melting ice on UAVs. The 3K and 6K Twill weaves show similar behavior where the heat spreads uniformly over the area between the two electrodes. In contrast, in the 12K Unidirectional weave the heat generated along the tows spreads less to the adjacent tows. Thus, the 3K and 6K Twill weaves are preferred for this integrated heater.

In addition, printing electronics on textiles is a challenge because of the large surface roughness of textiles. This paper presents a new method with the optimized parameters to use extrusion printing to print on textile composites, mainly carbon fiber weaves. The standoff distance between the nozzle and the textile needs to be increased to avoid entanglement between the nozzle and the fibers. To nevertheless achieve good print quality and sufficient ink flow, the piston pressure needs to be increased while compensating for the loss in pressure throughout a print run. As a result, the manufacturing of the carbon fiber-based heating devices is repeatable and scalable. Furthermore, since extrusion printing is a contactless digital printing method, the proposed methods allow for the facile variation of the pattern design to create various types of electronic devices and circuits.

Acknowledgements

We acknowledge funding support from York University through the Lassonde Innovation Fund (LIF).

References

[1] G. Grau, E. J. Frazier, and V. Subramanian, “Printed unmanned aerial vehicles using paper-based electroactive polymer actuators and organic ion gel transistors,” Microsystems Nanoeng., vol. 2, 2016.

[2] M. Ader and D. Axelsson, “Drones in arctic environments,” 2017.

[3] R. W. Gent, N. P. Dart, and J. T. Cansdale, “Aircraft icing,” Philos. Trans. R. Soc. A Math. Phys. Eng. Sci., vol. 358, no. 1776, pp. 2873–2911, 2000.

[4] A. Beisswenger, C. Laforte, and J. Perron, “Issues and testing of non-glycol aircraft ground deicing fluids,” in SAE Technical Papers, 2011.

[5] K. L. Sørensen, Autonomous Icing Protection Solution for Small Unmanned Aircraft: An Icing Detection, Anti-Icing and De-Icing Solution. 2016.

[6] P. Bhatt and A. Goe, “Carbon Fibres: Production, Properties and Potential Use,” Mater. Sci. Res. India, vol. 14, no. 1, pp. 52–57, Jun. 2017.

[7] X. Huang, “Fabrication and properties of carbon fibers,” Materials, vol. 2, no. 4. pp. 2369–2403, 2009.

[8] C. Ferro, R. Grassi, C. Seclì, and P. Maggiore, “Additive Manufacturing Offers New Opportunities in UAV Research,” in Procedia CIRP, 2016.

[9] S. Morton, R. D’Sa, and N. Papanikolopoulos, “Solar powered UAV: Design and experiments,” in IEEE International Conference on Intelligent Robots and Systems, 2015, vol. 2015-December, pp. 2460–2466.

[10] X. Yao, S. C. Hawkins, and B. G. Falzon, “An advanced anti-icing/de-icing system utilizing highly aligned carbon nanotube webs,” Carbon N. Y., vol. 136, pp. 130–138, Sep. 2018.

[11] L. Vertuccio, F. De Santis, R. Pantani, K. Lafdi, and L. Guadagno, “Effective de-icing skin using graphene-based flexible heater,” Compos. Part B Eng., vol. 162, pp. 600–610, Apr. 2019.

[12] Y. Ming, Y. Duan, S. Zhang, Y. Zhu, and B. Wang, "Self-heating 3D printed continuous carbon fiber/epoxy mesh and its application in wind turbine deicing," Polym. Test., vol. 82, Feb. 2020.

[13] O. Galao, L. Bañón, F. Baeza, J. Carmona, and P. Garcés, "Highly Conductive Carbon Fiber Reinforced Concrete for Icing Prevention and Curing," Materials (Basel)., vol. 9, no. 4, p. 281, Apr. 2016.

[14] H. Zhao, Z. Wu, S. Wang, J. Zheng, and G. Che, "Concrete pavement deicing with carbon fiber heating wires," Cold Reg. Sci. Technol., vol. 65, no. 3, pp. 413–420, Mar. 2011.

[15] M. Stoppa and A. Chiolerio, "Wearable electronics and smart textiles: A critical review," Sensors (Switzerland), vol. 14, no. 7. pp. 11957–11992, 07-Jul-2014.

[16] J. S. Chang, A. F. Facchetti, and R. Reuss, "A Circuits and Systems Perspective of Organic/Printed Electronics: Review, Challenges, and Contemporary and Emerging Design Approaches," IEEE J. Emerg. Sel. Top. Circuits Syst., vol. 7, no. 1, pp. 7–26, Mar. 2017.

[17] Y. Khan, A. Thielens, S. Muin, J. Ting, C. Baumbauer, and A. C. Arias, "A New Frontier of Printed Electronics: Flexible Hybrid Electronics," Adv. Mater., p. 1905279, Nov. 2019.

[18] H. F. Castro et al., "Degradation of all-inkjet-printed organic thin-film transistors with TIPS-pentacene under processes applied in textile manufacturing," Org. Electron., vol. 22, pp. 12–19, Jul. 2015.

[19] I. Kazani, C. Hertleer, G. de Mey, A. Schwarz, G. Guxho, and L. van Langenhove, "Electrical conductive textiles obtained by screen printing," Fibres Text. East. Eur., vol. 90, no. 1, pp. 57–63, 2012.

[20] A. E. Ostfeld, I. Deckman, A. M. Gaikwad, C. M. Lochner, and A. C. Arias, "Screen printed passive components for flexible power electronics," Sci. Rep., vol. 5, Oct. 2015.

[21] Y. Li, R. Torah, S. Beeby, and J. Tudor, "An all-inkjet printed flexible capacitor on a textile using a new poly(4-vinylphenol) dielectric ink for wearable applications," in Proceedings of IEEE Sensors, 2012, pp. 1–4.

[22] J. S. Chang, A. F. Facchetti, and R. Reuss, "A Circuits and Systems Perspective of Organic/Printed Electronics: Review, Challenges, and Contemporary and Emerging Design Approaches," IEEE J. Emerg. Sel. Top. Circuits Syst., vol. 7, no. 1, pp. 7–26, Mar. 2017.

[23] W. Tang et al., "Recent progress in printable organic field effect transistors," Journal of Materials Chemistry C, vol. 7, no. 4. Royal Society of Chemistry, pp. 790–808, 2019.

[24] Z. Stempien, E. Rybicki, T. Rybicki, and J. Lesnikowski, "Inkjet-printing deposition of silver electro-conductive layers on textile substrates at low sintering temperature by using an aqueous silver ions-containing ink for textronic applications," Sensors Actuators B Chem., vol. 224, pp. 714–725, Mar. 2016.

[25] K. B. Perez and C. B. Williams, "Combining additive manufacturing and direct write for integrated electronics - A review," in 24th International SFF Symposium - An Additive Manufacturing Conference, SFF 2013, 2013, pp. 962–979.

[26] K. Suganuma, "Printing Technology," 2014, pp. 23–48.

[27] M. G. Mohammed and R. Kramer, "All-Printed Flexible and Stretchable Electronics," Adv. Mater., vol. 29, no. 19, May 2017.

[28] D. Zhao, T. Liu, M. Zhang, R. Liang, and B. Wang, "Fabrication and characterization of aerosol-jet printed strain sensors for multifunctional composite structures," Smart Mater. Struct., vol. 21, no. 11, Nov. 2012.

[29] T. Augustin, "Structural health monitoring of carbon fiber reinforced polymers and carbon nanotube modified adhesive joints via electrical resistance measurement," pp. 1–127, 2018.

[30] T. Augustin, D. Grunert, H. H. Langner, V. Haverkamp, and B. Fiedler, "Online monitoring of surface cracks and delaminations in carbon fiber/epoxy composites using silver nanoparticle based ink," Adv. Manuf. Polym. Compos. Sci., vol. 3, no. 3, pp. 110–119, Jul. 2017.

[31] F. Heinrich and R. Lammering, “A numerical approach to simulate printed electronics on fiber reinforced composites,” PAMM, vol. 16, no. 1, pp. 135–136, Oct. 2016.

[32] F. Heinrich and R. Lammering, “An experimental investigation on the adhesion of printed electronics on fiber reinforced composites,” in 8th European Workshop on Structural Health Monitoring, EWSHM 2016, 2016, vol. 4, pp. 2949–2956.

[33] F. Heinrich, T. Genco, and R. Lammering, “On the mechanical behavior of a composite stiffener with inkjet-printed electronics,” in 9th European Workshop on Structural Health Monitoring, EWSHM 2018, 2018.

[34] I. Miccoli, F. Edler, H. Pfnür, and C. Tegenkamp, “The 100th anniversary of the four-point probe technique: The role of probe geometries in isotropic and anisotropic systems,” Journal of Physics Condensed Matter, vol. 27, no. 22. p. 223201, 2015.